

---

---

# Prospective Phase II Trial of Prognostication by <sup>68</sup>Ga-NOTA-AE105 uPAR PET in Patients with Neuroendocrine Neoplasms: Implications for uPAR-Targeted Therapy

Esben Andreas Carlsen<sup>1,2</sup>, Mathias Loft<sup>1,2</sup>, Annika Loft<sup>1,2</sup>, Anne Kiil Berthelsen<sup>1,2</sup>, Seppo W. Langer<sup>2-4</sup>, Ulrich Knigge<sup>2,5</sup>, and Andreas Kjaer<sup>1,2</sup>

<sup>1</sup>Department of Clinical Physiology and Nuclear Medicine & Cluster for Molecular Imaging, Copenhagen University Hospital – Rigshospitalet & Department of Biomedical Sciences, University of Copenhagen, Copenhagen, Denmark; <sup>2</sup>ENETS Neuroendocrine Tumor Center of Excellence, Copenhagen University Hospital–Rigshospitalet, Copenhagen, Denmark; <sup>3</sup>Department of Oncology, Copenhagen University Hospital – Rigshospitalet, Copenhagen, Denmark; <sup>4</sup>Department of Clinical Medicine, University of Copenhagen, Copenhagen, Denmark; and <sup>5</sup>Departments of Clinical Endocrinology and Surgical Gastroenterology, Copenhagen University Hospital–Rigshospitalet, Copenhagen, Denmark

The clinical course for patients with neuroendocrine neoplasms (NENs) ranges from indolent to highly aggressive. Noninvasive tools to improve prognostication and guide decisions on treatment are warranted. Expression of urokinase plasminogen activator receptor (uPAR) is present in many cancer types and associated with a poor outcome. Therefore, using an in-house–developed uPAR PET tracer [<sup>68</sup>Ga]Ga-NOTA-Asp-Cha-Phe-D-Ser-D-Arg-Tyr-Leu-Trp-Ser-OH (<sup>68</sup>Ga-NOTA-AE105), we aimed to assess uPAR expression in NENs. We hypothesized that uPAR expression was detectable in a significant proportion of patients and associated with a poorer outcome. In addition, as uPAR-targeted radionuclide therapy has previously proven effective in preclinical models, the study would also indicate the potential for uPAR-targeted radionuclide therapy in NEN patients. **Methods:** In a prospective clinical phase II trial, we included 116 patients with NENs of all grades, of whom 96 subsequently had uPAR PET/CT performed with evaluable lesions. PET/CT was performed 20 min after injection of approximately 200 MBq of <sup>68</sup>Ga-NOTA-AE105. uPAR target-to-liver ratio was used to define lesions as uPAR-positive when lesion SUV<sub>max</sub>-to-liver SUV<sub>mean</sub> ratio was at least 2. Patients were followed for at least 1 y to assess progression-free and overall survival. **Results:** Most patients had small intestinal NENs (*n* = 61) and metastatic disease (*n* = 86). uPAR-positive lesions were seen in 68% (*n* = 65) of all patients and in 75% (*n* = 18) of patients with high-grade (grade 3) NENs. During follow-up (median, 28 mo), 59 patients (62%) experienced progressive disease and 28 patients (30%) died. High uPAR expression, defined as a uPAR target-to-liver ratio above median, had a hazard ratio of 1.87 (95% CI, 1.11–3.17) and 2.64 (95% CI, 1.19–5.88) for progression-free and overall survival, respectively (*P* < 0.05 for both). **Conclusion:** When <sup>68</sup>Ga-NOTA-AE105 PET was used to image uPAR in patients with NENs, uPAR-positive lesions were seen in most patients, notably in patients with both low-grade and high-grade NENs. Furthermore, uPAR expression was associated with a worse prognosis. We suggest that uPAR PET is relevant for risk stratification and that uPAR may be a promising target for therapy in patients with NENs.

**Key Words:** urokinase plasminogen activator receptor (uPAR); neuroendocrine neoplasms; PET; prognosis; molecular imaging

J Nucl Med 2022; 63:1371–1377  
DOI: 10.2967/jnumed.121.263177

Neuroendocrine neoplasms (NENs) originate from the neuroendocrine cells and are found primarily in the gastrointestinal tract, pancreas, and lungs. The clinical course for patients diagnosed with NENs ranges from indolent to highly aggressive. The origin of the primary tumor, presence of metastases, tumor morphology, and proliferation activity (i.e., Ki-67) are known prognostic factors. Patients are stratified by the World Health Organization (WHO) classification into neuroendocrine tumor (NET) grade 1 (G1) (Ki-67, <3%), NET grade 2 (G2) (Ki-67, 3%–20%), NET grade 3 (G3) (Ki-67, >20% and well differentiated), and neuroendocrine carcinoma (NEC) (Ki-67, >20% and poorly differentiated) (1). To further improve prognostication and guide decisions on treatment, noninvasive monitoring of tumor markers may be useful. PET is ideally suited for this task, as different specific radiotracers may be applied to visualize whole-body expression of tumor markers noninvasively. In NENs particularly, radiotracers for somatostatin receptor expression (e.g., <sup>64</sup>Cu-DOTA-TATE or <sup>68</sup>Ga-DOTATATE) and glucose metabolism (<sup>18</sup>F-FDG) are useful for diagnosis, prognostication, and therapy selection (2,3). In addition, peptide receptor radionuclide therapy (PRRT) with, for example, <sup>177</sup>Lu-DOTATATE targeting somatostatin receptors is approved for low-grade NENs, whereas lower somatostatin receptor expression in high-grade NENs can limit its application.

Urokinase plasminogen activator receptor (uPAR) is a promising diagnostic and prognostic biomarker, as well as a target for therapy, and has been extensively investigated in several cancer entities (4). uPAR is anchored to the cell membrane on the surface and localizes the proteolytic activity of its ligand, urokinase plasminogen activator (uPA). In normal tissues, uPAR expression is limited; however, in cancer, uPAR expression is upregulated. Apart from uPA, uPAR also interacts with other proteins, among them the integrin family of membrane proteins. Collectively, uPAR is involved in promoting cell proliferation, motility, invasion, proteolysis, and angiogenesis (4–6). Because of its integral role in cancer, our group has developed the PET radiotracer [<sup>68</sup>Ga]Ga-NOTA-Asp-Cha-Phe-D-Ser-D-Arg-Tyr-Leu-Trp-Ser-OH (<sup>68</sup>Ga-NOTA-AE105) using a high-affinity

---

Received Sep. 14, 2021; revision accepted Jan. 12, 2022.  
For correspondence or reprints, contact Prof. Andreas Kjaer (akjaer@sund.ku.dk).  
Published online Jan. 20, 2022.  
COPYRIGHT © 2022 by the Society of Nuclear Medicine and Molecular Imaging.

antagonist for uPAR (7–9). Safety and biodistribution were investigated in a phase I study, also showing accumulation of <sup>68</sup>Ga-NOTA-AE105 in primary tumors and metastases, as well as correlation with uPAR expression in excised tumor samples (7). Recently, we reported that <sup>68</sup>Ga-NOTA-AE105 uPAR PET is able to discriminate between low-risk and intermediate-risk profiles in prostate cancer (10). Furthermore, we have previously shown a high efficacy of uPAR-targeted PRRT in preclinical trials in prostate and colorectal cancers (11,12). Thus, uPAR, being a marker of aggressive disease, may show upregulation in high-grade NENs and provide a target for PRRT in these patients.

The aim of this phase II clinical trial of <sup>68</sup>Ga-NOTA-AE105 PET/CT in patients with NENs was to assess tumor uptake and clinical outcome. We hypothesized that uPAR PET/CT with <sup>68</sup>Ga-NOTA-AE105 would show accumulation in NENs and that the uptake of the uPAR tracer would be associated with progression-free survival (PFS) and overall survival (OS).

## MATERIALS AND METHODS

### Patients

Patients with histologically confirmed NENs were included from the Department of Endocrinology (managing low-grade NENs; Ki-67, ≤20%) and the Department of Oncology (managing high-grade NENs; Ki-67, >20%) at Copenhagen University Hospital–Rigshospitalet between November 1, 2017, and May 29, 2020. Rigshospitalet is a certified Neuroendocrine Tumor Center of Excellence by the European Neuroendocrine Tumor Society. The study was conducted in accordance with the Helsinki Declaration and good clinical practice. The study was approved by the Danish Medicines Agency (EudraCT 2017-002312-13), the Scientific Ethics Committee (H-17019400), and the Danish Data Protection Agency (2012-58-0004) and was registered on clinicaltrials.gov (NCT03278275).

Eligible patients were more than 18 y old, able to read and understand the patient information in Danish, and able to give informed consent. They had to have a diagnosis of a gastroenteropancreatic NEN of any grade or a bronchopulmonary NEN and have a WHO performance status of 0–2. Patients were excluded if they were pregnant or breast-feeding, had a body weight of more than 140 kg, had a history of allergic reaction to compounds of similar chemical or biologic composition to <sup>68</sup>Ga-NOTA-AE105, or—in cases of bronchopulmonary NENs—had small cell lung cancer as the subtype. After written informed consent had been obtained, the patients were referred to undergo <sup>68</sup>Ga-NOTA-AE105 PET/CT at the first given opportunity.

### Image Acquisition

Data were acquired using a Biograph 128 mCT PET/CT device (Siemens Medical Solutions) with an axial field of view of 216 mm. On the basis of the previous phase I trial (7), the scan was acquired 20 min after intravenous administration of approximately 200 MBq of <sup>68</sup>Ga-NOTA-AE105. The tracer was produced as previously described (7). Whole-body PET scans (middle of orbita to middle of thigh) were acquired with a time of 4 min per bed position. Attenuation- and scatter-corrected PET data were reconstructed iteratively using a 3-dimensional ordinary Poisson ordered-subset expectation-maximization algorithm including point-spread function and time-of-flight information using the TrueX algorithm (Siemens Medical Solutions); the settings were 2 iterations, 21 subsets, and a 2-mm gaussian filter. A diagnostic CT scan was obtained before the PET scan, with a 2-mm slice thickness, 120 kV, and a quality reference of 225 mAs modulated by the Care Dose 4D automatic exposure control system (Siemens Medical Solutions). An automatic injection system was used to administer 75 mL of an iodine-containing contrast agent (Optiray 300; Covidien) for arterial- and venous-phase CT.

**TABLE 1**  
Baseline Characteristics of Patients with NENs (*n* = 96)

Characteristic	Data
Median age (y)	66 (range, 34–82)
Sex	
Female	39 (41%)
Male	57 (59%)
Site of primary tumor	
Small intestine	61 (64%)
Pancreas	15 (16%)
Colon	10 (10%)
Lung	6 (6%)
Esophagus	1 (1%)
Stomach	2 (2%)
Rectum	1 (1%)
Metastatic disease	86 (90%)
Liver metastases	73 (76%)
Median Ki-67	7 (range, 1–100)
WHO grade	
NET G1	21 (22%)
NET G2	51 (53%)
NET G3	9 (9%)
NEC	15 (16%)
Median time from diagnosis to uPAR PET/CT (mo)	25 (range, 0.5–265)
Primary tumor resected	37 (39%)
Ongoing treatment at uPAR PET/CT scan time*	
Somatostatin analog	70 (73%)
Interferon	8 (8%)
Carboplatin or etoposide	19 (20%)
Capecitabine/5-fluorouracil	6 (6%)
Streptozotocin	5 (5%)
Temozolomide	2 (2%)
Everolimus	2 (2%)
Completed treatment before uPAR PET/CT*	
On first line of therapy	45 (47%)
PRRT	28 (29%)
Temozolomide	6 (6%)
Capecitabine/5-fluorouracil	6 (6%)
Streptozotocin	5 (5%)
Carboplatin or etoposide	10 (10%)
Everolimus or sunitinib	2 (2%)
Interferon	6 (6%)
Liver radiofrequency ablation or embolization	5 (5%)
Resection of liver metastases	4 (4%)

\*Some patients had received more than one treatment; therefore, number of treatments exceed number of patients.

Data are number followed by percentage in parentheses, unless otherwise indicated. Percentages were rounded and may not add up to 100%.

**TABLE 2**  
Proportion of Patients with uPAR PET-Positive Tumors by WHO Grade

Parameter	G1 (n = 21)	G2 (n = 51)	G3 (n = 24)	Overall (n = 96)
uPAR PET-positive	12 (57%)	35 (69%)	18 (75%)	65 (68%)

Data are number followed by percentage in parentheses. uPAR TLR was used to define lesions as uPAR-positive when lesion  $SUV_{max}$ -to-normal-liver  $SUV_{mean}$  was  $\geq 2$ . Of patients with G3, 8 of 9 NET G3 and 10 of 15 NEC were uPAR PET-positive.

### Image Analysis

An experienced board-certified nuclear medicine physician together with an experienced board-certified radiologist analyzed side by side the PET/CT scans. The readers were masked to patient data. Lesions were identified on CT and/or PET. SUV was calculated as decay-corrected measured radioactivity concentration/(injected activity/body weight). If more than one lesion was present in an organ, the lesion with the highest  $^{68}\text{Ga}$ -NOTA-AE105  $SUV_{max}$  was noted. If no uPAR-positive lesions were identified, but lesions were visible on CT, the largest lesion (based on viable tumor) on CT was used as a guide for delineation on the PET scan and  $SUV_{max}$  was determined. Physiologic liver uptake was assessed in all patients' normal liver tissue, preferable on the right side of the liver, avoiding major blood vessels. To standardize measurement of uPAR expression within and between patients, uPAR target-to-liver

ratio (TLR) was used to define a lesion as uPAR-positive when lesion  $SUV_{max}$ -to-normal-liver  $SUV_{mean}$  ratio was at least 2.

### Follow-up

The patients were followed at the Rigshospitalet Neuroendocrine Tumor Center of Excellence with regular visits, including clinical examination, blood samples, and imaging (CT, MR, ultrasound, or PET/CT). The frequency was in accordance with European Neuroendocrine Tumor Society guidelines (13). Follow-up for endpoints was performed on July 8, 2021. Routine CT or MRI was used for evaluation of PFS in accordance with RECIST, version 1.1 (14). PFS was calculated as time from uPAR PET/CT to, if any, progression or death from any cause. If no progression or death from any cause occurred within the follow-up, the patient was censored at the time of the last available diagnostic imaging. OS was calculated as time from uPAR PET/CT to death by any cause. As all but 2 deaths were directly related to NENs, we refrained from analyzing disease-specific survival. Patients alive at follow-up were censored to the day of follow-up, that is, July 8, 2021.

### Statistics

Sample size was based on previous studies of prognostic markers in patients with NENs (15,16), where a 1-y follow-up of 100 patients

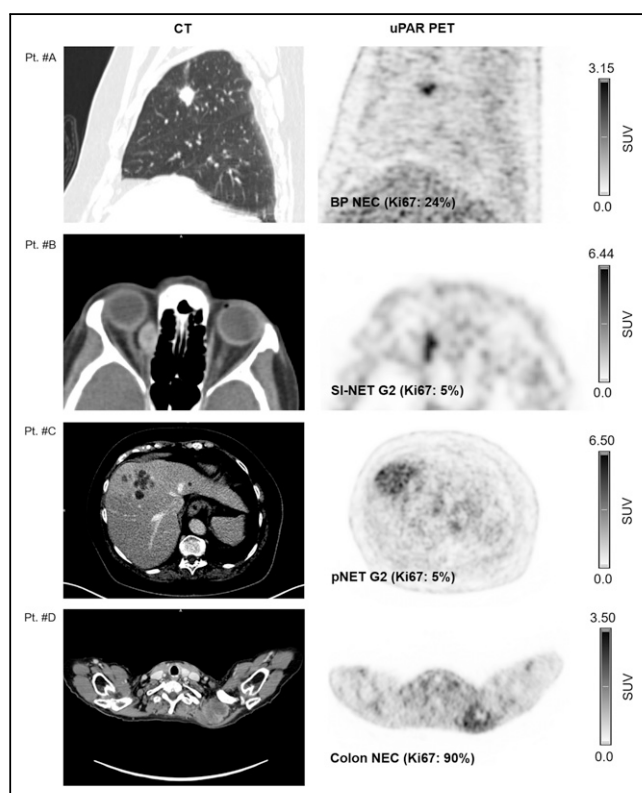


**FIGURE 1.** Representative examples of uPAR PET/CT imaging. CT (left column) and uPAR PET (right column) are shown for 4 patients (patients A–D) with high- and low-grade NENS. Top of individual scale bar corresponds to  $SUV_{max}$  of tumor. Pt. #A: Bronchopulmonary NEC (Ki67: 24%). Pt. #B: Orbital metastasis from small intestine NET G2 (Ki-67: 5%); Pt. #C: Large liver metastasis from pancreatic NET G2 (Ki-67: 5%). Pt. #D: Large intramuscular metastasis from primary colon NEC (Ki-67: 90%). BP = bronchopulmonary; SI = small intestine; pNET = pancreatic NET.

**TABLE 3**  
Treatment After uPAR PET/CT (n = 96)

Treatment	Data
Somatostatin analog	74 (77%)
Interferon	6 (6%)
PRRT	27 (28%)
Capecitabine/5-fluorouracil	10 (10%)
Everolimus or sunitinib	12 (13%)
Temozolomide	8 (8%)
Carboplatin or etoposide	11 (11%)
Streptozotocin	3 (3%)
Topotecan	2 (2%)
Docetaxel	2 (2%)
Irinotecan	1 (1%)
Surgery	9 (9%)
Liver embolization	7 (7%)
Liver radiofrequency ablation	2 (2%)
External radiation	11 (11%)

Some patients had received more than one treatment; therefore, number of treatments exceeds number of patients. Data are number followed by percentage in parentheses.

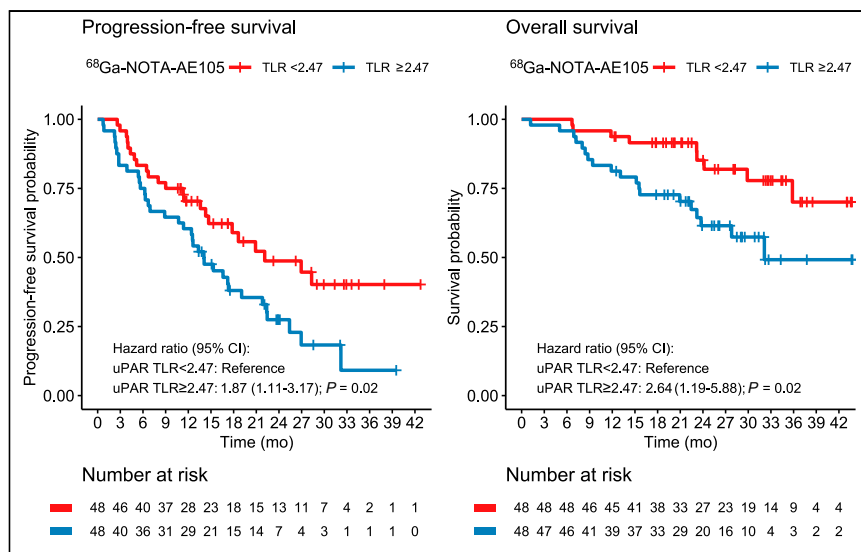


**FIGURE 2.** Kaplan–Meier plots of OS and PFS using  $^{68}\text{Ga}$ -NOTA-AE105 uPAR PET. uPAR TLR was dichotomized at median (TLR, 2.47).

was sufficient to detect significant differences in PFS and OS among groups (with a risk of type I error of 0.05 and power of 0.8). To account for dropouts, 116 patients were included. Continuous variables are reported as mean  $\pm$  SD or median with range. Kaplan–Meier analyses were used to estimate time to outcome (PFS and OS) and inverse Kaplan–Meier for median follow-up time. We used the Cutoff Finder application to determine the optimal cutoff for uPAR TLR (17). Univariate and multivariate Cox regression analyses for OS and PFS, with predictor variables of uPAR TLR and WHO grade, were performed. A *P* value of less than 0.05 was considered statistically significant. R, version 3.6.0 (R Foundation for Statistical Computing), was used for the analyses.

## RESULTS

### Patients and Image Acquisition

We prospectively included 116 patients, 17 of whom did not undergo uPAR PET/CT (worsening of disease, *n* = 5; withdrawal of consent, *n* = 5; death before uPAR PET/CT, *n* = 4; impossibility of performing uPAR PET/CT because of coronavirus disease 2019 restrictions, *n* = 3). Of 99 patients scanned with uPAR PET/CT, 96 had evaluable lesions (failure of uPAR PET/CT because of a technical issue, *n* = 1; lack of visible lesions on either CT or PET, *n* = 2). Patient demographic data for the study cohort (*n* = 96) are given in Table 1. Most patients had small intestinal NENs (64%, 61/96), and 90% (86/96) had metastatic disease. Also, patients with high-grade disease were well represented in the cohort, with 9% NET G3 (9/96) and 16% NEC (15/96).

Patients were injected with a median of 17.2  $\mu\text{g}$  (range, 8.7–39.8  $\mu\text{g}$ ) of  $^{68}\text{Ga}$ -NOTA-AE105, and the activity was 194 MBq (range, 104–236 MBq). The time from injection to the PET scan was a median of 22 min (range, 18–38 min). One patient experienced an adverse event (mild nausea), which was deemed unrelated to  $^{68}\text{Ga}$ -NOTA-AE105 injection. No serious adverse events were recorded.

### Image Analysis

Tracer uptake in normal liver tissue was used as a reference for tumor uptake. The mean ( $\pm$ SD) normal-liver  $\text{SUV}_{\text{mean}}$  was  $1.50 \pm 0.39$ . uPAR-positive lesions were seen in both patients with low-

grade NEN (NET G1/G2) and patients with high-grade NEN (NET G3 and NEC) (Table 2). Representative examples of uPAR PET are shown in Figure 1 and Supplemental Fig. 1 (supplemental materials are available at <http://jnm.snmjournals.org>).

### Follow-up

The median follow-up time after uPAR PET/CT was 28 mo. During follow-up, 59 (62%) patients experienced progressive disease (median, 17.3 mo) and 28 patients (30%) died. The patients' treatments after uPAR PET/CT are shown in Table 3. Treatment with a somatostatin analog was the most frequent (77%, 74/96), and 28% (27/96) of patients underwent PRRT during follow-up.

### PFS and OS

uPAR TLR as a continuous variable was significantly associated with PFS, with an HR of 1.27 (95% CI, 1.02–1.60; *P* = 0.04). For OS, uPAR TLR as a continuous marker was borderline-significant, with an HR of 1.37 (95% CI, 0.98–1.92; *P* = 0.06). TLR was then dichotomized at the median value (2.47) for Kaplan–Meier analyses (Fig. 2). Median OS was not reached in the group with low uPAR expression (TLR < median) and was 32.1 mo (95% CI, 23.8–upper limit not reached) in the group with high uPAR expression (TLR  $\geq$  median). Median PFS was 22.1 mo (95% CI, 14.7–upper limit not reached) in patients with low uPAR expression and 14.1 mo (95% CI, 11.4–22.4) in patients with high uPAR expression. uPAR TLR dichotomized at median was significantly associated with PFS and OS; patients with high uPAR expression had a significantly worse prognosis (Tables 4 and 5). Other cutoffs were evaluated using Cutoff Finder, shown in Supplemental Figure 2. When a lower cutoff for TLR (1.32) was used, a smaller group of patients (*n* = 10) with no or a very low risk of death or progression could be identified (Fig. 3). Patients with NET G3 and NEC had significantly worse PFS and OS than patients with NET G1, whereas no difference was seen between NET G2 and NET G1 (Tables 4 and 5). In multivariate analyses including uPAR expression and WHO classification, both remained significantly associated with PFS, whereas uPAR expression had a borderline-significant association with OS (*P* = 0.06) when we controlled for WHO grade.

## DISCUSSION

Our major finding in this prospective phase II study of  $^{68}\text{Ga}$ -NOTA-AE105 uPAR PET was that uPAR expression was seen in most patients with both low-grade and high-grade NENs. Furthermore, high uPAR expression was associated with a worse prognosis with regard to both PFS and OS. These findings imply that uPAR could be an attractive target for therapy both because of the availability of the target in patients with NENs and because of the possibility of specifically targeting the lesions associated with a poorer prognosis.

The role of uPA and uPAR in cancer has been extensively investigated in the last few decades, and it is well established that higher uPAR expression is associated with tumor growth, invasiveness, and metastatic spread, although this has not been

**TABLE 4**  
Uni- and Multivariate Cox Regression Analyses for PFS

PFS	Univariate Cox		Multivariate Cox	
	HR	<i>P</i>	HR	<i>P</i>
<b>uPAR TLR*</b>				
Low	Reference	—	Reference	—
High	1.87 (1.11–3.17)	0.02	1.75 (1.02–2.99)	0.04
<b>WHO grades</b>				
NET G1	Reference	—	Reference	—
NET G2	1.21 (0.57–2.55)	0.62	1.26 (0.59–2.66)	0.55
NET G3	4.16 (1.52–11.36)	<0.01	3.56 (1.29–9.82)	0.01
NEC	4.26 (1.82–9.95)	<0.001	4.43 (1.89–10.39)	<0.001

\*Dichotomized at median (2.47).  
HR = hazard ratio.  
Data in parentheses are 95% CIs.

thoroughly investigated in patients with NENs (18). Accordingly, several therapies targeting uPA and uPAR are undergoing investigation, such as a uPAR antibody (huATN-658) (19) and a serine protease inhibitor targeting uPA (upamostat) (20). However, none of these therapies has yet been approved for clinical use.

Patients with NENs have highly varying aggressiveness of disease. The primary tumor site, presence of metastases, and WHO classification are important prognostic markers and used to guide selection of treatment (21). Our group and others have shown that, in addition, low somatostatin receptor density as determined by <sup>64</sup>Cu-DOTATATE PET and high glucose metabolism as determined by <sup>18</sup>F-FDG PET are prognostic factors (2,3,16,22). With the concept of tailored treatments, specific tumor markers are used to guide eligibility for targeted treatments. This concept has seen widespread implementation in the treatment of patients with NENs, with somatostatin receptor imaging being used as a companion to screen for eligibility for somatostatin receptor-targeted therapy with <sup>177</sup>Lu-DOTATATE. In a randomized trial of patients

receiving <sup>177</sup>Lu-DOTATATE compared with a high dose of cold somatostatin analog treatment, the former group had significantly fewer deaths, a longer PFS, and an 18% response rate (23). One drawback of targeting somatostatin receptor-expressing tumors is the fact that lower expression of somatostatin receptors is seen with less differentiated and more aggressive tumors (24). In contrast, uPAR expression is particularly seen in lesions showing tumor growth, invasiveness, and metastatic capability. Previously, our group has investigated uPAR expression by immunohistochemical staining of primary tumor or metastasis from patients with NEN G3 (Ki-67, >20%), showing uPAR expression in stromal or tumor cells in 16 of 21 (76%) patients (25). However, to the best of our knowledge, expression of uPAR in patients with low-grade NENs has never been studied in situ but has been studied only indirectly by measurement of soluble uPAR (suPAR) in serum (26). suPAR is the cleaved version of the membrane-bound uPAR and may thus be measured as a circulating uPAR biomarker. The study reported higher levels of suPAR in NEN

**TABLE 5**  
Uni- and Multivariate Cox Regression Analyses for OS

OS	Univariate Cox		Multivariate Cox	
	HR	<i>P</i>	HR	<i>P</i>
<b>uPAR TLR*</b>				
Low	Reference	—	Reference	—
High	2.64 (1.19–5.88)	0.02	2.23 (0.96–5.20)	0.06
<b>WHO grades</b>				
NET G1	Reference	—	Reference	—
NET G2	1.40 (0.29–6.76)	0.67	1.59 (0.33–7.70)	0.56
NET G3	9.94 (2.00–49.52)	0.01	7.82 (1.55–39.44)	0.01
NEC	15.55 (3.49–69.37)	<0.001	17.09 (3.80–76.81)	<0.001

\*Dichotomized at median (2.47).  
HR = hazard ratio.  
Data in parentheses are 95% CIs.



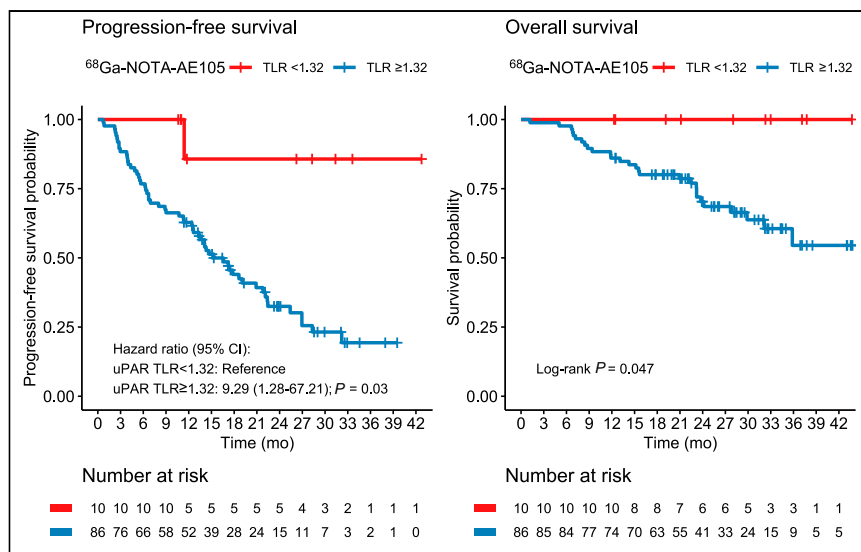


**FIGURE 3.** Kaplan-Meier plots of OS and PFS using  $^{68}\text{Ga}$ -NOTA-AE105 uPAR PET. uPAR TLR was dichotomized at 1.32.

patients than in healthy controls, as well as elevated levels of suPAR in both patients with low-grade disease and patients with high-grade disease. However, no association between suPAR levels and OS was seen. Contrary to that study, using PET to visualize uPAR expression at the tumor level is a more direct approach, making it possible to identify the lesions with the greatest uPAR expression and their location. Also, the expression pattern of uPAR has previously been shown to be heterogeneous, with uPAR being highly expressed at the margin of the tumor and thus locally promoting tissue invasion and seeding of metastases, a hallmark of cancer (27). In support of this observation, we found that high uPAR expression on PET was associated with a worse prognosis, both with regard to PFS and with regard to OS. In line with our previous observations in patients with NEC and the data on suPAR in NENs, we found uPAR expression to be present in both low-grade and high-grade NENs. Hence, uPAR-targeted treatment may be relevant in patients with NENs of all grades. Our observations on uPAR expression should be viewed in light of the fact that the patients included in this study had mainly small intestinal or pancreatic primary tumors with metastatic disease and were previously treated.

A potential innovative perspective is to combine uPAR PET imaging and uPAR PRRT as a theranostic pair, hence using uPAR PET to assess eligibility for uPAR-targeted therapy. We have previously shown a high efficacy of uPAR PRRT in preclinical models of human prostate and colorectal cancer (11,12); however, further studies are warranted to assess the use of uPAR PRRT within NENs. The first step toward uPAR PRRT for NENs was to provide evidence for a high and specific uptake of our uPAR-targeting radioligand and the prognostic implications in NENs, as done in the present study.

## CONCLUSION

uPAR expression assessed by  $^{68}\text{Ga}$ -NOTA-AE105 PET is seen in most patients with both low-grade and high-grade NENs, and high uPAR expression is associated with a worse prognosis with regard to both PFS and OS. Collectively, this finding points to uPAR as a relevant target to pursue for risk stratification and possibly also for targeted therapy in patients with NENs.

## DISCLOSURE

This project received funding from the European Union's Horizon 2020 Research and Innovation Program under grants 670261 (ERC Advanced Grant) and 668532 (Click-It), the Lundbeck Foundation, the Novo Nordisk Foundation, the Innovation Fund Denmark, the Danish Cancer Society, the Arvid Nilsson Foundation, the Neye Foundation, Novartis Health Care, the Research Foundation of Rigshospitalet, the Danish National Research Foundation (grant 126), the Research Council of the Capital Region of Denmark, the Danish Health Authority, the John and Birthe Meyer Foundation, the Research Council for Independent Research, and the Neuroendocrine Tumor Research Foundation. Andreas Kjaer is a Lundbeck Foundation Professor, inventor on a patent of the composition of matter of uPAR PET (WO 2014086364), and co-founder of Curasight, which has licensed the

uPAR PET technology. No other potential conflict of interest relevant to this article was reported.

## ACKNOWLEDGMENT

We are grateful to our dedicated colleagues at the Departments of Clinical Physiology, Nuclear Medicine, and PET; Endocrinology; and Oncology, Rigshospitalet, for assistance with patient recruitment, radiotracer production, and PET/CT acquisition. We express our sincere gratitude to all the patients who participated in the study.

## KEY POINTS

**QUESTION:** Is uPAR expression seen in patients with NENs and associated with prognosis?

**PERTINENT FINDINGS:** Using  $^{68}\text{Ga}$ -NOTA-AE105 for uPAR PET/CT imaging, we saw uPAR expression in most NEN patients, including both high-grade and low-grade NENs. Furthermore, increased uPAR expression, both as a continuous variable and dichotomized at median, was associated with increased hazard for progression of disease and death.

**IMPLICATIONS FOR PATIENT CARE:** uPAR PET imaging may be useful for risk stratification in patients with NENs. Furthermore, uPAR may be a possible treatment target given the expression of uPAR across patients with both high-grade and low-grade NENs and given that uPAR expression is associated with a poor outcome.

## REFERENCES

- Klimstra DS, Kloppel G, La Rosa S, Rindi G. *Digestive System Tumours*. 5th ed. International Agency for Research on Cancer; 2019:16–19.
- Carlsen EA, Johnbeck CB, Loft M, et al. Semiautomatic tumor delineation for evaluation of  $^{64}\text{Cu}$ -DOTATATE PET/CT in patients with neuroendocrine neoplasms: prognostication based on lowest lesion uptake and total tumor volume. *J Nucl Med*. 2021;62:1564–1570.
- Binderup T, Knigge U, Johnbeck CB, et al.  $^{18}\text{F}$ -FDG PET is superior to WHO grading as a prognostic tool in neuroendocrine neoplasms and useful in guiding PRRT: a prospective 10-year follow-up study. *J Nucl Med*. 2021;62:808–815.

4. Mahmood N, Rabbani SA. Fibrinolytic system and cancer: diagnostic and therapeutic applications. *Int J Mol Sci.* 2021;22:4358.
5. Ahn SB, Mohamedali A, Pascovici D, et al. Proteomics reveals cell-surface urokinase plasminogen activator receptor expression impacts most hallmarks of cancer. *Proteomics.* 2019;19:e1900026.
6. Mahmood N, Mihalciou C, Rabbani SA. Multifaceted role of the urokinase-type plasminogen activator (uPAR) and its receptor (uPAR): diagnostic, prognostic, and therapeutic applications. *Front Oncol.* 2018;8:24.
7. Skovgaard D, Persson M, Brandt-Larsen M, et al. Safety, dosimetry, and tumor detection ability of <sup>68</sup>Ga-NOTA-AE105: first-in-human study of a novel radioligand for uPAR PET imaging. *J Nucl Med.* 2017;58:379–386.
8. Persson M, Madsen J, Ostergaard S, Ploug M, Kjaer A. <sup>68</sup>Ga-labeling and in vivo evaluation of a uPAR binding DOTA- and NODAGA-conjugated peptide for PET imaging of invasive cancers. *Nucl Med Biol.* 2012;39:560–569.
9. Kriegbaum MC, Persson M, Haldager L, et al. Rational targeting of the urokinase receptor (uPAR): development of antagonists and non-invasive imaging probes. *Curr Drug Targets.* 2011;12:1711–1728.
10. Fosbøl MØ, Kurbegovic S, Johannesen HH, et al. Urokinase-type plasminogen activator receptor (uPAR) PET/MRI of prostate cancer for noninvasive evaluation of aggressiveness: comparison with Gleason score in a prospective phase 2 clinical trial. *J Nucl Med.* 2021;62:354–359.
11. Persson M, Rasmussen P, Madsen J, Ploug M, Kjaer A. New peptide receptor radionuclide therapy of invasive cancer cells: in vivo studies using <sup>177</sup>Lu-DOTA-AE105 targeting uPAR in human colorectal cancer xenografts. *Nucl Med Biol.* 2012;39:962–969.
12. Persson M, Juhl K, Rasmussen P, et al. uPAR targeted radionuclide therapy with <sup>177</sup>Lu-DOTA-AE105 inhibits dissemination of metastatic prostate cancer. *Mol Pharm.* 2014;11:2796–2806.
13. Knigge U, Capdevila J, Bartsch DK, et al. ENETS consensus recommendations for the standards of care in neuroendocrine neoplasms: follow-up and documentation. *Neuroendocrinology.* 2017;105:310–319.
14. Eisenhauer EA, Therasse P, Bogaerts J, et al. New response evaluation criteria in solid tumours: revised RECIST guideline (version 1.1). *Eur J Cancer.* 2009;45:228–247.
15. Johnbeck CB, Knigge U, Langer SW, et al. Prognostic value of <sup>18</sup>F-FLT PET in patients with neuroendocrine neoplasms: a prospective head-to-head comparison with <sup>18</sup>F-FDG PET and Ki-67 in 100 patients. *J Nucl Med.* 2016;57:1851–1857.
16. Binderup T, Knigge U, Loft A, Federspiel B, Kjaer A. <sup>18</sup>F-fluorodeoxyglucose positron emission tomography predicts survival of patients with neuroendocrine tumors. *Clin Cancer Res.* 2010;16:978–985.
17. Budczies J, Klauschen F, Sinn BV, et al. Cutoff Finder: a comprehensive and straightforward web application enabling rapid biomarker cutoff optimization. *PLoS One.* 2012;7:e51862.
18. Li Santi A, Napolitano F, Montuori N, Ragno P. The urokinase receptor: a multifunctional receptor in cancer cell biology: therapeutic implications. *Int J Mol Sci.* 2021;22:4111.
19. Mahmood N, Arakelian A, Khan HA, Tanvir I, Mazar AP, Rabbani SA. uPAR antibody (huATN-658) and Zometa reduce breast cancer growth and skeletal lesions. *Bone Res.* 2020;8:18.
20. Heinemann V, Ebert MP, Laubender RP, Bevan P, Mala C, Boeck S. Phase II randomised proof-of-concept study of the urokinase inhibitor upamostat (WX-671) in combination with gemcitabine compared with gemcitabine alone in patients with non-resectable, locally advanced pancreatic cancer. *Br J Cancer.* 2013;108:766–770.
21. Janson ET, Knigge U, Dam G, et al. Nordic guidelines 2021 for diagnosis and treatment of gastroenteropancreatic neuroendocrine neoplasms. *Acta Oncol.* 2021;60:931–941.
22. Carlsen EA, Johnbeck CB, Binderup T, et al. <sup>64</sup>Cu-DOTATATE PET/CT and prediction of overall and progression-free survival in patients with neuroendocrine neoplasms. *J Nucl Med.* 2020;61:1491–1497.
23. Strosberg J, El-Haddad G, Wolin E, et al. Phase 3 trial of <sup>177</sup>Lu-Dotatate for midgut neuroendocrine tumors. *N Engl J Med.* 2017;376:125–135.
24. Sorbye H, Kong G, Grozinsky-Glasberg S. PRRT in high-grade gastroenteropancreatic neuroendocrine neoplasms (WHO G3). *Endocr Relat Cancer.* 2020;27:R67–R77.
25. Olsen IH, Langer SW, Federspiel BH, et al. <sup>68</sup>Ga-DOTATOC PET and gene expression profile in patients with neuroendocrine carcinomas: strong correlation between PET tracer uptake and gene expression of somatostatin receptor subtype 2. *Am J Nucl Med Mol Imaging.* 2016;6:59–72.
26. Özdirik B, Stueven A, Knorr J, et al. Soluble urokinase plasminogen activator receptor (suPAR) concentrations are elevated in patients with neuroendocrine malignancies. *J Clin Med.* 2020;9:1647.
27. Hanahan D, Weinberg RA. Hallmarks of cancer: the next generation. *Cell.* 2011;144:646–674.